The Mechanism of the Storm Surges in the Seto Inland Sea Caused by Typhoon Chaba (0416)

Nadao KOHNO

Typhoon Research Department, Meteorological Research Institute,
1-1Nagamine, Tsukuba 305-0052, Japan

Kazuo KAMAKURA, Hiroaki MINEMATSU*, Yukihiro YORIOKA,
Kazuhisa HISASHIGE, Eichi SHIMIZU, Yuichi SATO,
Akifumi FUKUNAGA, Yoshihiko TANIWAKI, and Shigekazu TANIJO

Observation and Forecast Division, Takamatsu Local Observatory,
1277-1 Fuki-ishi, Takamatsu 761-8071, Japan

Abstract

Typhoon Chaba in 2004 made landfall on the southeastern Kyushu and went through Chugoku (western part of Japan's Main Island) on 30 August, causing large storm surges in the Seto Inland Sea (SIS). The high tide records were broken at tide stations in Takamatsu and Uno Ports. We analyzed the tidal data and simulated this case with a numerical storm surge model.

The storm surges moved eastward along with the passage of the typhoon, and it was favorably simulated. The results revealed that the wind set-up basically played a key role in causing the large storm surges. However, the maximum storm surge (MSS) in Takamatsu did not occur when the typhoon was the nearest to the city, but about 2 hours later. Since the time of MSS approximately corresponds to the high spring tide time, the record breaking storm tide was observed there.

Moreover, we found the SIS can be divided into 6 areas according to the characteristics of sea topography and dominant wind direction by the typhoon. We also investigated the degrees of the contribution of two main factors of storm surges, i.e. inverted barometric effect and wind set-up, in each area. As a result, it turned out that the peak times of each effect were influenced by the geographical feature, as well as the wind field and the position of the typhoon, and had different characters in each area.

*Present affiliation: Marine Division, Japan Meteorological Agency

This report is basically an English-translated paper from an article in the bulletin Journal "Tenki" of Meteorological Society of Japan (MSJ).

1. Introduction

Storm surges generated by typhoons have often brought large disasters in the coast of Japan. Especially, in the case of Typhoon (TY) Vera, which caused 5,098 dead or missing in 1959, most of the casualties were brought by the storm surges. The countermeasures to storm surges have developed progressively after this disaster. However, serious storm surges still occurred. In 1991, large storm surges were generated in the western part of the Seto Inland Sea (SIS; shown in Fig. 1) by TY Mireille (Konishi, 1994; Konishi and Tsuji, 1995). However, severe disaster did not occur since the maximum storm surge (MSS) occurred just in low tide. In 1999, the storm surges by TY Bart led to serious disasters; 13 people were directly killed by storm surges in Yatsushiro Sea, and Yamaguchi-Ube airport in the Suoh-Nada (western part of the SIS) was unavailable by inundation (JMA, 2000; Kohno, 2000). The tracks of these two typhoons are almost the same and both of them generated large storm surges in Yatsushiro Sea. Recently, intense typhoons have frequently hit Japan since 2000, and serious disasters sometimes happened. In 2004, as many as ten named tropical cyclones made landfall on Japan, which is quite extraordinary since usual number is two or three. Several tropical cyclones brought disasters due to storm surges. Especially, TY Chaba generated large storm surges in the SIS, and the coincidence of MSS with the peak time of high tide caused the highest storm tide records at Takamatsu and Uno (central part of the SIS). More than 8,300 houses are inundated above the floor level only in Kagawa Prefecture, and total damages were quite enormous as 16,799 houses inundated above the floor level.

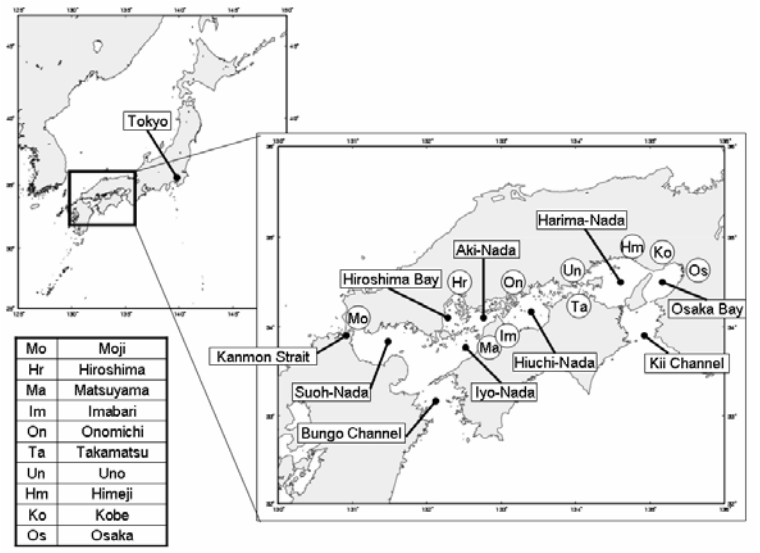

Fig. 1 Map of the western part of Japan and the Seto Inland Sea (SIS). The whole area of the Seto Inland Sea from the Suoh-Nada to the Osaka Bay is an inland sea. The points of tide stations are also shown.

Although large storm surges sometimes occurred in the SIS due to typhoon passages as mentioned above, most cases happened in the Suoh-Nada (western part of the SIS) or the Osaka-Bay (eastern part of the SIS), and they rarely occurred in the central part of the SIS. TY Chaba is applicable to the latter case. This case is also characterized by the fact that the MSS occurred a few hours later than the time when the typhoon was

nearest. Therefore we have investigated the mechanism of this storm surge with a concern to the effects of sea topography and the sequence of typhoon position, mainly based on a numerical model.

TY Chaba and storm surges in the SIS are described in section 2, and the outline of the simulation and the results are provided in section 3. Section 4 focuses on the factors that may mainly contribute to storm surges, and the conclusion is summarized in section 5.

2. TY Chaba (0416) and storm surges in the SIS

2.1 TY Chaba (0416)

A tropical depression (TD) was formed in the sea around the Caroline Islands at 06UTC (all times are expressed in UTC hereafter) on 18 August 2004. It moved slowly westward and developed into a Tropical Storm Chaba at 12UTC on 19 August. Chaba continued to move westward and was upgraded into a Typhoon at 18UTC on 21 August. Then it turned toward the northwest at the southwestern edge of sub-tropical high on 23 August. The typhoon continuously intensified during this period and developed to the strongest level as central pressure of 910hPa and the maximum wind speed of 56m/s at 18UTC on 23 August.

The typhoon kept its intensity till 18UTC on 26 August, moving to northwest and gradually weakened. The typhoon moved to west again in the sea east of the Nansei Inlands and turned to the north-northeast in the sea south of Kyushu.

The typhoon made landfall at Kushikino at about 00UTC on 30 August, with central pressure 950hPa, the maximum wind speed 41m/s, and the radius of storm wind extended to 230km east (Fig. 2). The typhoon passed through Kyushu and moved northward in the Suoh-Nada, and made landfall again at around Hohfu. As the TY Chaba approaching, Chugoku, Shikoku, northern and central part of Kinki were gradually covered by storm winds. The typhoon passed Tottori at about 12UTC with slightly

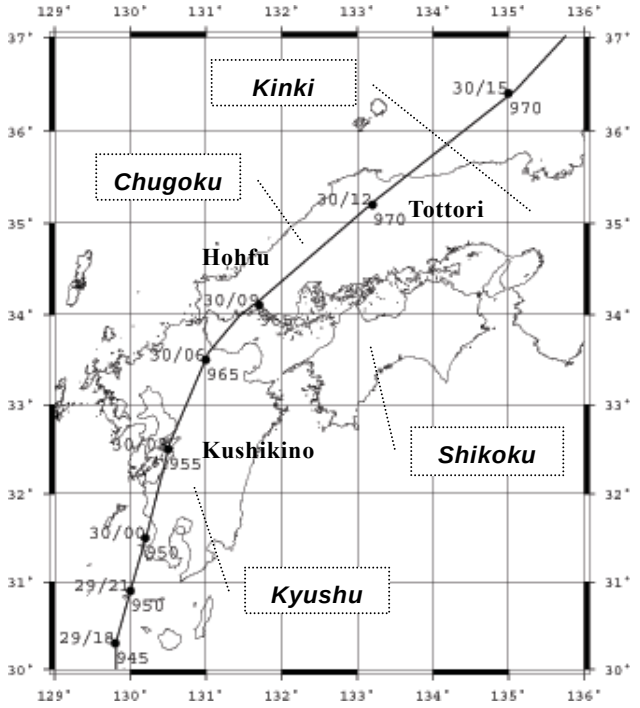

Fig. 2 Best track of TY Chaba (0416). The circles on the path indicate the positions of the typhoon every 3 hours. Days and hours (UTC) are plotted to the upper left and central pressures (hPa) to the lower right of each point.

weakened intensity (central pressure 960hPa and the maximum wind speed of 31m/s), and became to move faster in the Sea of Japan. The typhoon made landfall again at Hakodate at 03UTC on 31 August, and transformed into an extratropical cyclone in the east of Hokkaido at 06UTC.

Strong winds were observed in the areas the typhoon passed nearby. In Okayama, the maximum wind of 21.1m/s (SW) and the maximum gust of 38.5m/s (SW) were observed at 15:20 and 12:51UTC on 30 August, respectively; those were the highest records there. The positions and intensities of TY Chaba from 06UTC on 29 to 15UTC on 30 August are listed in Table 1.

Table 1 The positions and intensities of TY Chaba from 06UTC on 29/Aug/2004 to 15UTC on 30/Aug/2004.

Date and Time(UTC)	Lat. (deg.)	Lon. (deg.)	Ps (hPa)	Max Wind (m/s)
Aug/29 0600	28.3	130.7	940	44
Aug/29 0900	28.7	130.3	940	44
Aug/29 1200	29.0	130.1	940	44
Aug/29 1500	29.3	129.9	940	41
Aug/29 1800	29.8	129.8	945	41
Aug/29 2100	30.3	129.8	945	41
Aug/30 0000	30.9	130.0	950	41
Aug/30 0300	31.5	130.2	950	41
Aug/30 0600	32.5	130.5	955	41
Aug/30 0900	33.5	131.0	965	36
Aug/30 1200	33.9	131.4	965	36
Aug/30 1500	34.1	131.7	965	36

2.2 Storm surges in the SIS by TY Chaba

The main storm surges in the SIS by TY Chaba occurred from 30 to 31 August. Fig. 3 shows the time series of hourly storm surges (the each storm surge is defined by detracting astronomical tide from observed sea level) observed at tide stations. The magnitudes of the MSSs are generally about 1-1.5m.

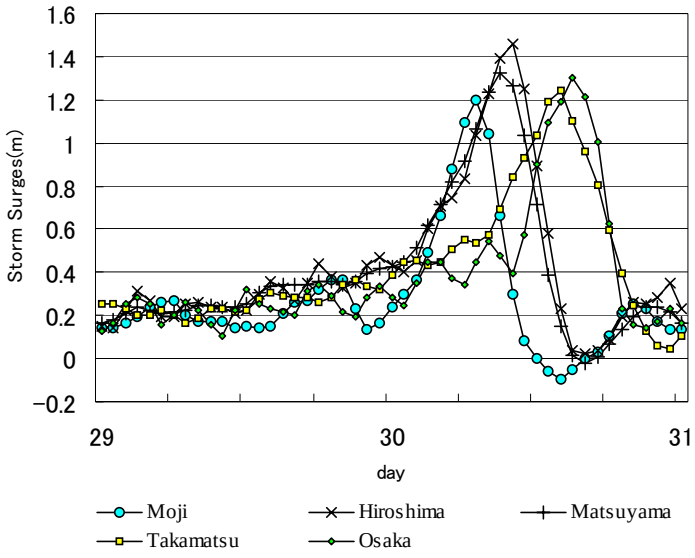

Fig. 3 Storm surges observed at several tide stations in the Seto Inland Sea.

The more east the observation point is located,

the later the MSS was observed. (Table 2). For example, in the western part of the SIS, the MSS of 1.33m in Moji was observed at 06:36. The MSSs in Hiroshima and Matsuyama occurred at 09:35 (1.49m) and 08:49 (1.40m), respectively. MSSs in Takamatsu and Uno were observed after 13UTC, 4 hours later than that in Matsuyama. The MSS of 1.33m was observed at 13:23 in Takamatsu, and 1.37m at 13:16 in Uno. In Kobe and Osaka, that are in the eastern part of the SIS, the MSSs were observed just before 15UTC: 1.34m at 14:42 in Kobe and 1.32m at 14:30 in Osaka.

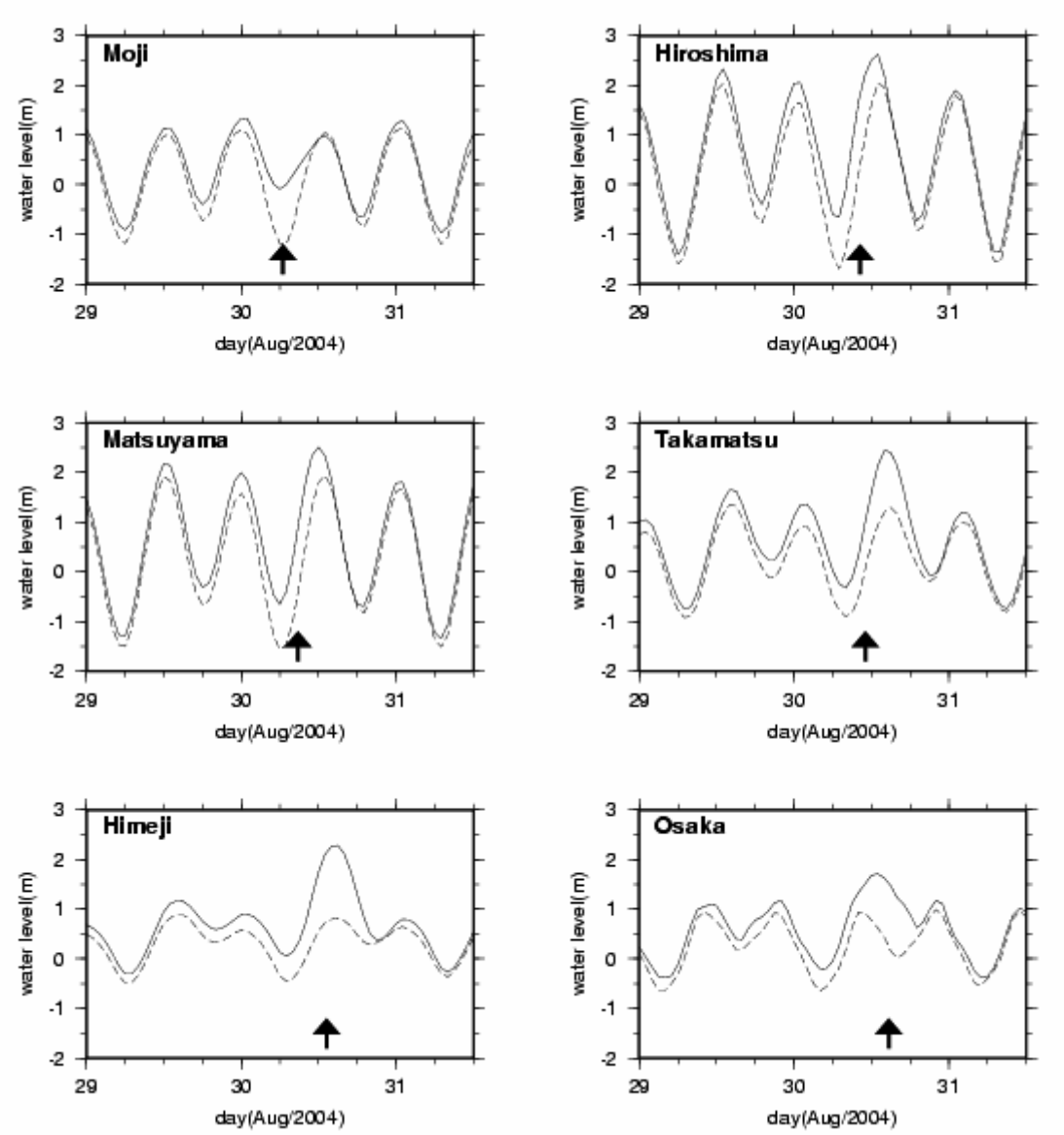

Fig. 4 The observed sea levels at several tide stations in the Seto Inland Sea. The observed sea levels are indicated by a solid line; the broken line represents the astronomical tide. The arrows show the time of the minimum surface pressure.

Fig. 4 shows the water levels at several tide stations. The magnitudes of the storm surges are not so different among these points, but the magnitudes of the storm tides are different each other because the timing of the astronomical tides are different

each other. Since the time of MSSs were the same as that of low tide in Moji, storm tides did not become so high; the maximum tides were observed about 6 hours earlier than the time of MSS (around 00:30), this was mostly contributed by high tide, not the storm surge. The maximum storm tides of 2.58m (Matsuyama) and 2.69m (Hiroshima) were observed at 11:56 and 12:56 respectively, 2-3 hours earlier than the high tides. The maximum storm tide there results from combination of storm surge and astronomical tide. The maximum storm tides were observed in Takamatsu and Uno at 13:42 and 13:47, respectively, only 30 minutes later than MSS. Moreover, since it was period of spring tide, water levels at high water were higher than usual. This also led to the highest record of maximum tides as 2.46m (Takamatsu) and 2.54m (Uno). This extraordinary high storm tide caused enormous disasters, and more than 12,000 houses were flooded to over floor level in these coastal areas. The maximum storm tides were observed at 12:24 in both Kobe and Osaka to the east of Takamatsu, which was about 2 hours earlier than the time of MSSs.

Table 2 The maximum storm surges (MSS), the minimum sea level pressures (MSLP) and the difference of time.

Tide station	MSS (m) and time (UTC)	MSLP (hPa) and time(UTC)	difference of time (min.)
Moji	1.33 (06:36)	969.5 (06:30)	6
Hiroshima	1.49 (09:35)	972.1 (10:16)	-41
Matsuyama	1.40 (08:49)	972.8 (08:49)	—
Uno	1.37 (13:16)	978.1 (10:48)	148
Takamatsu	1.33 (13:23)	978.1 (11:01)	132
Himeji	1.57 (14:50)	982.7 (13:13)	97
Kobe	1.34 (14:42)	987.5 (14:05)	37
Osaka	1.32 (14:30)	988.1 (13:42)	48

In order to investigate the relation of storm surges to the relative position of typhoon, the time of MSS and the time when the minimum sea level pressure (MSLP) was observed, which corresponds to the time when the typhoon mostly approached, are listed in Table 2. The easterly wind was predominant in the western part of the SIS as the typhoon was approaching, and the sea level became higher from early stage in the Suoh-Nada. Around the Suoh-Nada area, the times of MSSs were almost the same as the time of the MSLP, since the typhoon passed through the Suoh-Nada. For example, in Moji, the time of MSS (1.33m) was only 6 minutes later than MSLP time. After the typhoon passed and made landfall at Chugoku region, the predominant wind turned to westerly in the wake of typhoon, and large storm surge area shifted to the eastern part of the SIS gradually. The MSS was observed at almost the same time of MSLP in Matsuyama, but was 41 minutes earlier in Hiroshima. At the points to the east of Matsuyama, the MSSs were observed later than the time of the MSLP.

It is notable that the times of MSS in Takamatsu and Uno were more than 2 hours

later than the times of the MSLPs, but in Himeji and Osaka, located in further east of Uno, the difference of times between MSS and MSLP became smaller again. This indicates that the storm surge area did not move monotonously to east while the typhoon was simply leaving northward.

3. Numerical simulation with storm surge model

3.1 Outline of the storm surge model and numerical methods

The basic equations of the storm surge model are momentum flux and continuity of water mass under the rotating field with gravitational acceleration.

$$\begin{aligned}\frac{\partial Du}{\partial t}+\frac{\partial Du^2}{\partial x}+\frac{\partial Duv}{\partial y}&=-\frac{g}{\rho_w}D\frac{\partial(\varsigma-\varsigma_0)}{\partial x}-\frac{1}{\rho_w}(\tau_{ax}-\tau_{bx})+fDv\\ \frac{\partial Dv}{\partial t}+\frac{\partial Duv}{\partial x}+\frac{\partial Dv^2}{\partial y}&=-\frac{g}{\rho_w}D\frac{\partial(\varsigma-\varsigma_0)}{\partial y}-\frac{1}{\rho_w}(\tau_{ay}-\tau_{by})-fDu\end{aligned} \tag{3.1}$$

$$\frac{\partial \varsigma}{\partial t}+\frac{\partial Du}{\partial x}+\frac{\partial Dv}{\partial y}=0 \tag{3.2}$$

where (x, y) shows horizontal direction, $\mathbf{U} = (u, v)$ current components, ζ height deviation, ζ_0 balance level with surface pressure, ρ_w sea water density, f Coriolis parameter, and g gravitational acceleration. D shows the local water depth.

The surface stress $\boldsymbol{\tau}_\mathbf{a} = (\tau_{ax}, \tau_{ay})$ by winds and the bottom stress $\boldsymbol{\tau}_\mathbf{b} = (\tau_{bx}, \tau_{by})$ are estimated with surface winds $\mathbf{V} = (v_x, v_y)$ and $\mathbf{U}$ as follows:

$$\begin{aligned}\boldsymbol{\tau}_\mathrm{a} &= -\rho_a C_{da}|\mathbf{V}|(v_x, v_y)\\ \boldsymbol{\tau}_\mathrm{b} &= -\rho_w C_{db}|\mathbf{U}|(u, v)\end{aligned} \tag{3.3}$$

where ρ_a is air density, C_{da} and C_{db} indicate the drag coefficients and their values are defined empirically as

$$\begin{aligned}C_{da} &= 3.2\times10^{-3}\\ C_{db} &= 2.5\times10^{-3}\end{aligned} \tag{3.4}$$

The coastal boundary was assumed to be a “rigid wall”, and no inundation or dry-up were considered. The boundary of open sea was assumed to maintain a static balance with the surface pressure, and a deviation from the statically balanced level makes inflow or outflow current as a gravitational wave.

The surface pressure field P_s is defined by the formula of Fujita (1952), using the parameters of the 3 hourly JMA best track data,

$$P_s(r) = P_\infty - \frac{P_\infty - P_c}{\sqrt{1+(r/r_0)^2}} \tag{3.5}$$

where P_c is the central pressure, P_∞ the environmental pressure and assumed to be

constant as 1012hPa. The parameter $r_{0,}$ which indicates typhoon size, is determined from substituting the radius of 1000hPa in a weather chart to (3.5).

The gradient wind derived from this profile gives the symmetrical surface wind, and the surface wind is defined to be asymmetrical by adding a typhoon moving speed to this gradient wind with a constant inflow angle of 30 degrees. The surface stress is obtained by substituting this surface wind to **V** in (3.3).

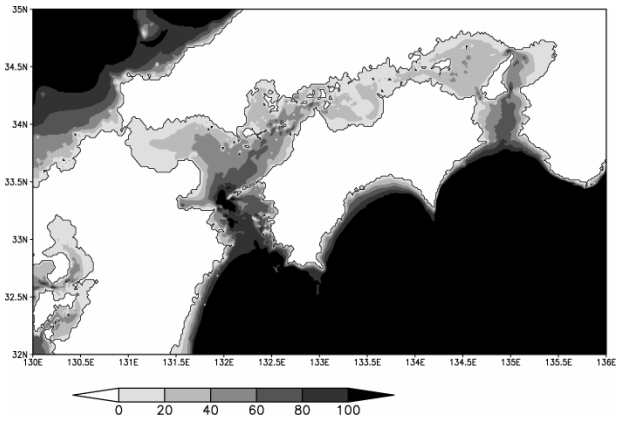

Fig. 5 The computational domain and water depth (m).

The computational area was set from 32°N to 35°N and from 130°E to 136°E, which covers the whole SIS, and the horizontal grid resolution was 1 minute (corresponds to a physical distance of 1.85km in latitude and 1.55km in longitude). The domain and sea topography used in the calculation are shown in Fig. 5. The calculation time step was 2 seconds, which completely satisfies the CFL condition since even the largest water depth does not exceed 1,000m. This grid resolution was not enough to express the Kanmon Straight, and sea water could not pass through. However, the gross characteristic of the storm surge in the SIS is supposed to be expressed adequately since the amount of sea water flow via channels such as the Bungo Channel, which is well represented, is far larger than that of the Kanmon Straight.

We conducted the simulation from the static initial state. Considering the earlier part being spent for spin up, we started the calculation from 00UTC on 29 August, two days before the typhoon hit the SIS.

3.2 Simulation results

Fig. 6 (a) shows the simulated storm surge distributions as well as the surface winds used in the calculations. The observation of winds is not so dense in this area, especially in the sea, for intensive comparison. Therefore, the surface winds of the hourly objective analysis, which is based on the operational Meso-Scale Model (MSM) prediction as a first guess and modified with the wind profiler observation, and shown in Fig. 6 (b), will be used for discussion in the next section. Although the hourly objective analysis does not represent the true atmosphere sufficiently, we assume that it is more realistic than the wind field derived from eq. (3.5).

Storm surges are little detected in the whole area before the typhoon reached Kyushu and a gale wind started. In the Suoh-Nada, large storm surge area is generated by strong easterly wind ahead of the approaching typhoon (06UTC on 30 August). As the

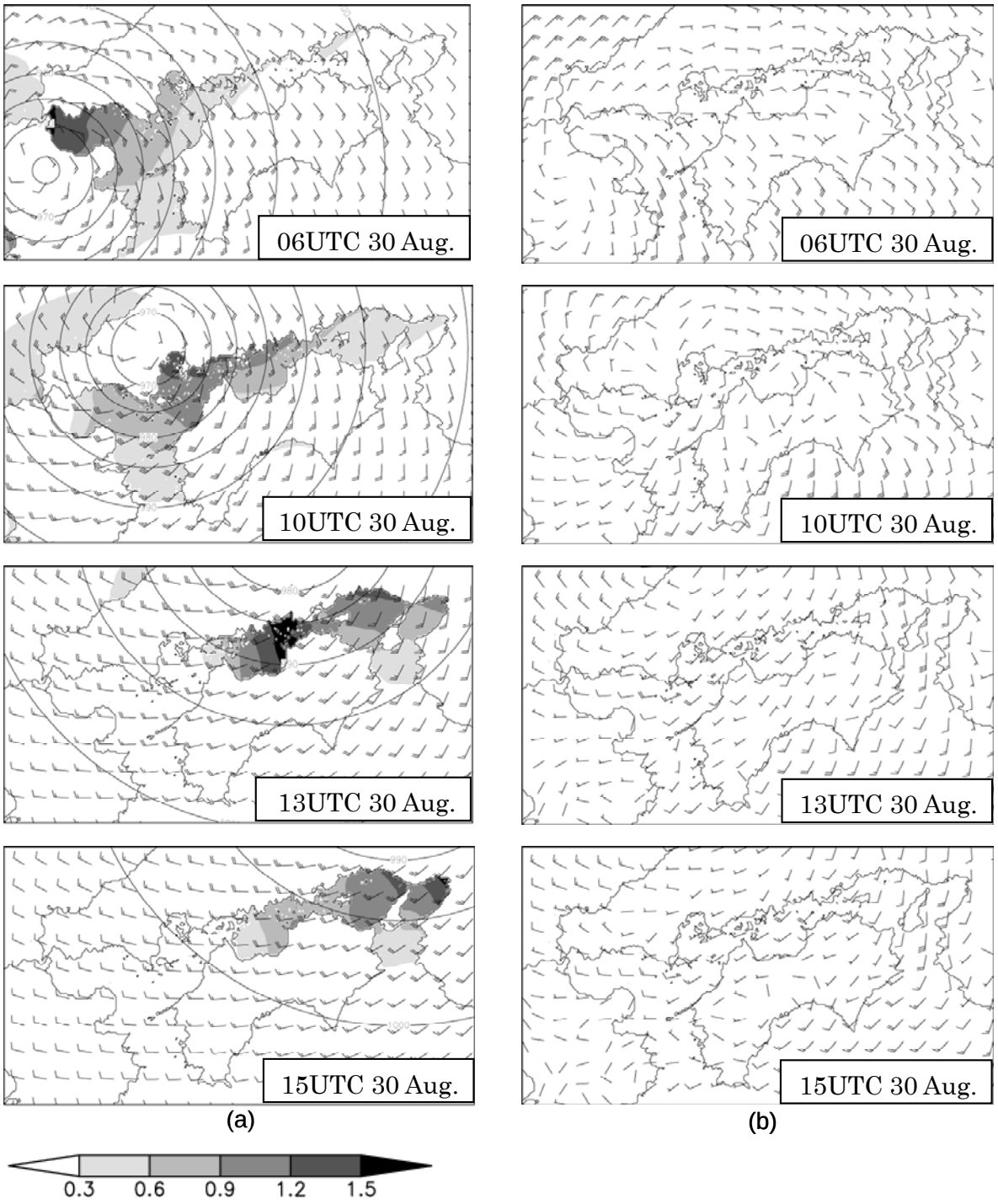

Fig. 6 Horizontal distribution of (a)the simulated storm surge and the model wind, and (b) the surface wind of the hourly objective analyses. The shades indicate simulated storm surges (m), and the contours in the left column show the model surface pressure. The barbs in both columns show the winds (long fletching is 10m/s, and short 5m/s).

typhoon had passed the Suoh-Nada and moved northeastward, the wind turned to westerly, which led the large storm surge area to move eastward (10UTC). Around 13UTC, although the typhoon had already moved away northward, a large storm surge is notable in the central sea to the west of a narrow straight (just where Takamatsu and Uno

exist). After that, although the typhoon continued to leave further, westerly wind continued to blow, and storm surge shifted eastward, to the Osaka Bay around 15UTC on 30 August.

The calculated MSSs at several points are listed in Table 3, and Fig. 7 shows the time series at Takamatsu: Observed and calculated storm surges, observed sea level pressures as well as those used in the model. According to Tables 2 and 3, all the calculated MSSs are favorably compared with observation and every error are within 0.30m. However, there are almost 1 hour differences in peak time at some points. This may mainly come from the error of meteorological data input, e.g. assumed pressure field given with eq. (3.5), since the time of minimum surface pressure given to the model is different from that of observation as shown in Fig. 7. The difference of pressure fields may also lead to the error of wind fields, but the wind fields in the time of MSS at Takamatsu was preferably estimated as shown in Fig. 6.

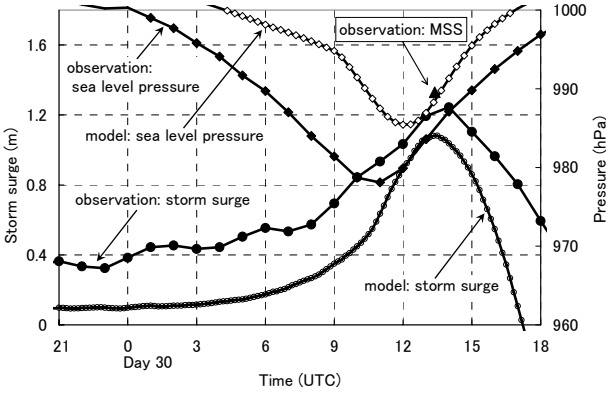

Fig. 7 The time series at Takamatsu

Table 3 The results of three calculations. Simulated magnitudes of the maximum storm surges (MSS), given MSLP with the occurrence time in parenthesis. Contribution ratio of the wind set-up in the MSS, CR, defined as the MSS in II divided by that in I is also listed.

Tide station	MSS(m) in I	MSLP (hPa)	MSS (m) in II	MSS (m) in III	CR
Moji	1.61 (05:40)	969 (07:20)	1.35 (05:20)	0.52 (08:40)	84%
Hiroshima	1.44 (10:10)	969 (10:20)	1.01 (08:50)	0.70 (11:10)	66%
Matsuyama	1.15 (10:30)	978 (10:00)	0.70 (10:20)	0.50 (11:00)	60%
Uno	1.19 (12:40)	983 (12:00)	0.89 (12:20)	0.49 (14:00)	74%
Takamatsu	1.08 (13:30)	985 (12:00)	0.76 (12:50)	0.47 (14:20)	69%
Himeji	1.47 (13:50)	985 (13:20)	1.16 (13:30)	0.46 (15:20)	78%
Kobe	1.40 (14:30)	990 (13:40)	1.11 (14:20)	0.36 (15:50)	79%
Osaka	1.62 (14:40)	991 (14:00)	1.35 (14:30)	0.37 (15:50)	82%

4. Discussion

Generally speaking, storm surges are mainly caused by two factors: the inverted

barometric effect and the wind set-up (e.g. Miyazaki, 2003). Both of the effects are easily estimated to some extent by assuming the static balance. In addition, it is known that, as Arakawa and Yoshitake (1935) pointed out, the dynamical effects such as resonance of the moving speed of meteorological disturbance and surface water movement as ocean long wave may cause large storm surges.

Since the numerical simulation model enables to include such dynamical effects without any simplification of topography, we will be able to proceed to discuss how the two main effects functioned in the simulation.

To detect these effects, we carried out two additional simulations: One is that only the wind effects are considered by setting the pressure force in the second term on the right side of (3.1) to $\zeta_0 = 0$ (hereafter we refer to as the "wind calculation"), and the other is that only the pressure effects are considered by setting the wind stress in the third term on the right side of (3.1) to τ_a to 0 (hereafter we refer to as the "pressure calculation"). We represent I as the control calculation, II as the "wind calculation", and III as the "pressure calculation". The MSSs by every calculation are listed in Table 3.

4.1 The inverted barometric effect

The results of III show that all the MSSs appeared after the time when the typhoon was nearest; especially the delay became large in the Hiuchi-Nada and the Osaka Bay, that is, Uno, Takamatsu, Himeji, Kobe and Osaka. The reason is supposed that the eastward movement of water piled up in the western part of the SIS was prevented at the narrow part of the east channel surrounded by the ellipse in Fig. 8 (a). In order to verify this hypothesis, a calculation with an experimental topography as shown in Fig. 8 (b) was conducted. (The channel part is enlarged and changed to the sea with 20m depth.) The result showed that the times of the MSS in the west of the Iyo-Nada were hardly changed. On the one hand, those in the east of the Iyo-Nada became earlier and the delay of time decreased (not shown). For example, the time became earlier about 20 minutes in Takamatsu and Uno, and about 40 minutes in the Hiuchi-Nada at most.

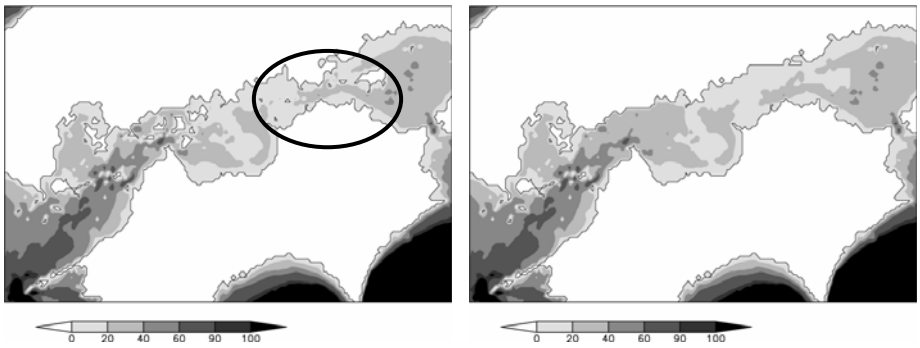

(a) (b)

Fig. 8 (a) The original topography, (b) The test one where the east channel is extended.

If the static balance (≒1cm/hPa) is assumed, the amount of surge by inverted

barometric effect can be estimated to be 30 - 40cm from the minimum surface pressure, that are generally 10cm smaller than the MSSs of III. The reason of this difference may be that sea water was preferably piled up, due to the inertia of sea water and the narrow strait as an “obstacle”. Therefore, the dynamical inverted barometric effect with an influence of sea topography is likely to give larger MSS than only static one would give in this area.

4.2 The wind set-up

The wind set-up is the major effect of the large storm surges. The “contribution ratio” of the wind set-up in the MSS defined as the MSS in II divided by that in I, (hereafter CR) was calculated in several tide station points. CR shows high value in every point as 70 - 80% (except Matsuyama of 60%). This indicates that the wind change along with a moving typhoon had an important role.

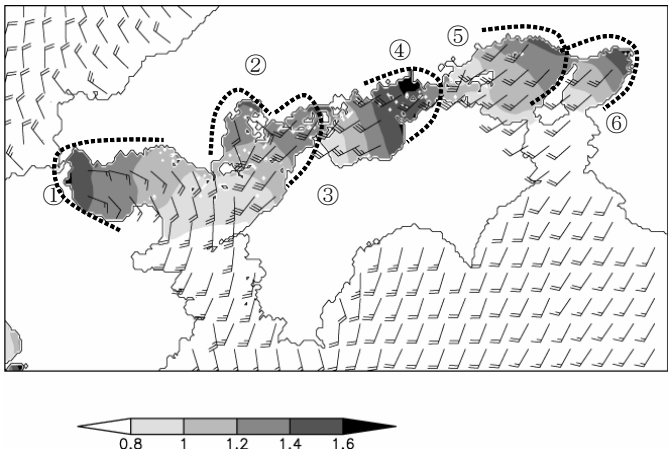

Fig. 9 The maximum storm surges (m) calculated in every grid and wind at same time

4.3 The characteristic differences among local seas

Fig. 9 shows the amplitudes of the MSS at every grid point and surface wind corresponding to the occurrence time of the calculation I. This distribution reveals several clusters of large storm surge area and wind direction. The storm surge in each area behaves as if the area is a bay, where large storm surge is generated in the most inner part by an inflow wind. By considering this characteristic, we divide the SIS into 6 local seas as shown in Fig. 9.

① the sea opening to east with the Kanmon Straight as a wall (the Suoh-Nada)
② the sea opening to south with the north coast of Hiroshima (the Hiroshima Bay)
③ the sea opening to southwest, closed by islands around Imabari (the Iyo-Nada and the Aki-Nada)
④ the sea opening to west, closed by the narrow channels (the Hiuchi-Nada)
⑤ the sea opening to south with the north coast of Himeji (the Harima-Nada)
⑥ the sea opening to south with the north coast of Osaka (the Osaka Bay)

Fig. 10 depicts the time series of the model sea level pressure and the storm

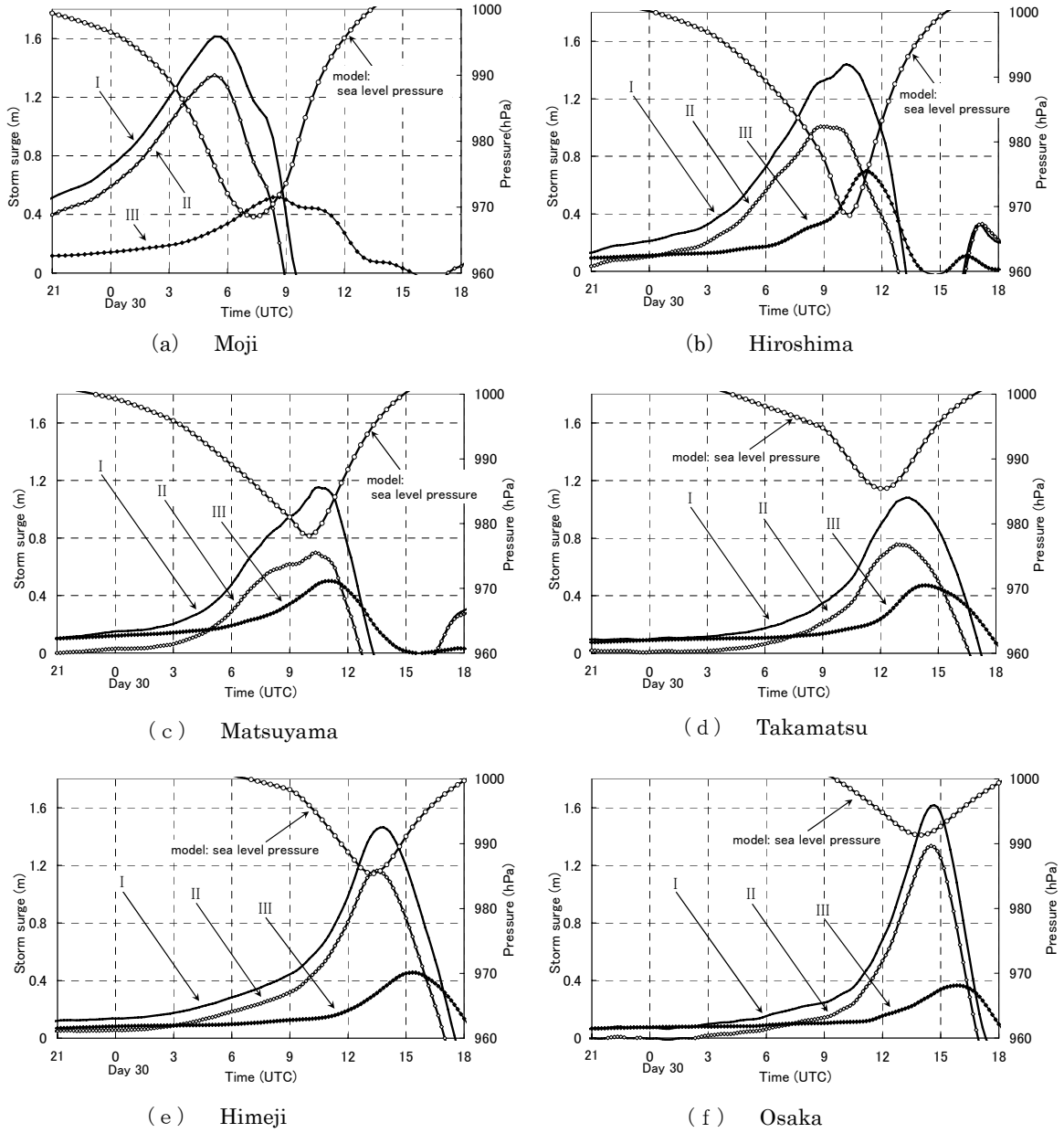

Fig. 10 The time series of calculation results in each area. The surface pressure (hPa) and calculated storm surges (m) by the cases of I, II, and III.

surges in calculations I, II, and III at a point of each sea. We describe on the characteristic points in every sea.

① the Suoh-Nada (tide station: Moji)

At Moji, the MSS of 1.33m was observed at 06:36 (Table 2), while 1.61m at 05:40 in calculation (Fig. 10a and Table 3). According to the hourly objective analyses in Fig. 6, easterly wind of 15m/s blow at the time of peak surge, which agrees with the model wind. The storm surge was generated mainly by this easterly wind. Since the effect of wind set-up can be estimated as follows if we assume a static balance:

$$\Delta z \propto \frac{\tau}{\rho_w g D} \cdot L \approx \frac{\rho_a C_{da} U^2}{\rho_w g D} \cdot L \,.$$

The surge anomaly Δz is proportional to stress τ, horizontal scale L, and the inverse of water depth D. The water depth in the Suoh-Nada is shallower than other seas as shown in Fig. 5, which lead to the largest CR of 84%. In addition, the southerly wind at the Bungo Channel induces large amount of sea water inflow to the Suoh-Nada. An additional calculation with the closed Bungo Channel reveals that the MSSs decreased by 0.13m at Moji and 0.30m at Tokuyama (eastern part of the Suoh-Nada) without inflow through the Bungo Channel.

Therefore, the storm surge in the Suoh-Nada is explained mainly by the wind set-up of easterly wind ahead of the typhoon, and the sea water provided via the Bungo Channel enlarged it.

② the Hiroshima Bay (Hiroshima)

At Hiroshima, the MSS of 1.49m was observed at 09:35 (Fig. 3 and Table 2), which is favorably simulated by the calculation of 1.44m at 10:10 (Fig. 10b and Table 3). The wind of hourly objective analyses shows 15 - 25m/s (S - SSW) during 09 to 10UTC, when the MSS occurred. The wind given to the model is almost the same, though the wind direction is rather S to SW. The storm surges in the Hiroshima Bay are explained by the wind set-up of this southerly wind. The wind turned to SW from SE as the typhoon moved northeastward, but it kept southerly direction, which was preferable for large storm surge.

③ the Iyo-Nada and the Aki-Nada (Matsuyama)

At Matsuyama, the MSS of 1.40m was observed at 08:49 (Fig. 3 and Table 2), while the MSS of 1.15m is calculated later at 10:30 (Fig. 10c and Table 3). According to the hourly objective analyses, the wind at the Iyo-Nada was about 15m/s (SW - SSW) around 09UTC, but the direction of model wind was southerly and the MSS occurred after the wind turned to SW. The fact that the time of the MSS coincides with the SW wind suggests that the MSS occurs when SW wind is predominant, and the coast around Imabari works as if it is a wall.

CR is the lowest (60%) among 8 tide station points because of its deep water depth. The contribution of the inverted barometric effect is relatively higher at Matsuyama than at other areas.

④ the Hiuchi-Nada (Takamatsu)

At Takamatsu, the MSS of 1.33m was observed at 13:23 (Fig. 3 and Table 2),

which is favorably simulated by the calculation of 1.08m at 13:30 (Fig. 10d and Table 3). The result at Uno was also reasonable. The wind during 13 to 14UTC, when the MSSs were observed at Takamatsu and Uno in the Hiuchi-Nada, was about 20m/s (WSW-SW) by both of the hourly objective analyses and wind given by the model, which caused similar storm surges by the wind set-up of westerly wind, and the peak was generated in the part to the west of the narrow channel between Uno and Takamatsu. The maximum of the inverted barometric effect appeared about 2 hours later than the minimum surface pressure. The reason of the delay is that flow of the sea water was reduced by the narrow east edge of the Aki-Nada.

The dominant wind direction is south while Takamatsu is open northward. Therefore, it is not reasonable to explain this storm surge simply by the local wind set-up. There may be possibility of any seiche being excited by own topography scale, but no such oscillation is detected. We consider that the storm surges in the Hiuchi-Nada was caused mainly by the accumulation of sea water, prevented from moving eastward at the narrow channel between Takamatsu and Uno.

According to a simulation with the channel between Imabari and Onomich being closed to reduce the inflow from the Aki-Nada, storm surges occurred but the maximum value decreased by 0.3 to 0.5m. This supports the speculation that the sea water from the Aki-Nada contributed to the storm surge in the Hiuchi-Nada.

⑤ the Harima-Nada (Himeji)

At Himeji, the MSS of 1.57m was observed at 14:50 (Fig. 3 and Table 2), while the calculation was 1.47m at 13:50 (Fig. 10e and Table 3). The CR is as high as 78% and the wind set-up by SW wind generated the storm surges in the Harima-Nada. Since the model wind agrees well with the wind of hourly objective analyses of 15-30m/s (S-SSW), and this sea opens southward and southwestward equally, the simulated result agrees well with the observation. Although the east Harima-Nada is connected to the Kii Channel via the Naruto Strait, the inflow of sea water through the narrow strait is supposed to be negligible.

⑥ the Osaka Bay (Osaka and Kobe)

At Osaka, the MSS of 1.32m was observed at 14:30 (Fig. 3 and Table 2), and 1.34m was observed at 14:42 at Kobe (Table 2). The calculation was 1.62m at 14:40 at Osaka (Fig. 10f and Table 3), 1.40m at 14:30 at Kobe (Table 3). The wind direction given by the model is different from that of the hourly objective analyses. The wind given by the model was southwesterly, and the MSS at Osaka was larger than that at Kobe due to its longer fetch. On the contrary, the wind of hourly objective analyses was southerly, which gives the same fetch both to Osaka and Kobe, and the MSSs were the same

magnitude. Since the water depth in the Osaka Bay is shallow, CR at Osaka and Kobe is as high as 79 – 82%.

Therefore the storm surge in the Osaka Bay as well as the Harima-Nada was mainly caused by the wind set-up of S – SW winds.

4.4 The further factors which may cause errors between calculation and observation

The calculation results show good agreement with observation, but there are still different points.

At first, the simulated amplitude of MSS at Moji is larger by 30cm than observed. This may be mainly because that Moji is located rather in the Kanmon Strait, not in the Suoh-Nada. The storm surge at Moji should be decreased by the water flow in this narrow Strait. A test calculation with exaggerated expression of wider strait led to an underestimation of storm surge, but storm surges calculated with closed strait showed much similar tendency to observation in quality. This suggests that the storm surge at Moji could be regarded as the phenomena at the western edge of the Suoh-Nada.

It should be also noted that the wind given by the model was about 10m/s larger than the hourly objective analyses, and the wind direction given by the model and that by the hourly objective analysis were, respectively, easterly and northerly. This might also lead to the larger storm surge by the model. This problem is also raised in the Osaka Bay as mentioned in the previous subsection.

Next, the MSS in Hiroshima occurred about 40 minutes later than that in Matsuyama, although Matsuyama is located to the east of Hiroshima. It seems to be mainly because Hiroshima is located in the most inner part of the bay. It took much time for waters to reach Hiroshima since Bohyo Islands are located in the SW of the Hiroshima Bay. Sea water seems to be prevented from moving northward by these islands.

The predominant wind direction was also different in the Kii Channel; the wind direction in the hourly analyses was bent to south by the topography. This may also lead to the errors in the Osaka Bay.

All of these problems essentially come from the wind fields, which are deduced from the ideal profiles of pressure approximated with eq. (3.5). The real structure of a typhoon is so complicated and the wind in the core area is far from being uniquely determined. Moreover, the wind is modulated by the topography, and the wind distribution is usually not simple. The “errors” of wind fields surely bring error in storm surges estimation. Therefore, a storm surge simulation with more realistic winds should be developed.

5. Conclusion

The mechanism of the storm surges in the SIS caused by TY Chaba in 2004 was investigated and our conclusions are summarized as follows:

(1) The storm surges by TY Chaba are mainly caused by the wind set-up effect.

(2) The SIS is divided into six areas in terms of the characteristics of the storm surge caused by TY Chaba. Each area is characterized by the preferred wind direction, relative importance of wind set-up effect and piling up of the sea water.

a. The Suoh-Nada

The wind set-up is extremely predominant due to its shallow water depth. The inflow of sea water from the Bungo Chanel also influences on the storm surges.

b. The Hiroshima Bay

Since the typhoon passed nearby and the duration of southerly wind was long, the wind set-up continued longer than other areas.

c. The Iyo-Nada

The wind set-up is not so predominant due to deep water. However, the coincidence of the time of the maximum inverted barometric effect and that of the wind set-up causes large storm surge.

d. The Hiuchi-Nada

The peak of inverted barometric effect appeared after the typhoon approached to the nearest because of the pile up of the sea water in the Aki-Nada. The coincidence of the time of the maximum inverted barometric effect and that of the wind set-up causes large storm surge similar to the Iyo-Nada.

e. The Harima-Nada and the Osaka Bay

The wind set-up functioned well since the sea opens to south and southwest and water depth is shallow.

(3) The time of the MSS was different among the areas. The time is almost the same as the time when the typhoon was nearest in the western part, although it delayed in the eastern part, especially the delay of time in the Hiuchi-Nada was over 2 hours. This indicates that storm surges in the SIS have good chances to occur after a typhoon passing away by the influence of sea topography. The timing of MSS was also influenced by the change of wind directions along with the typhoon movement.

Since it is rather common for a typhoon to pass along the same course as TY Chaba, that made landfall in Kyushu and passed into the Sea of Japan, it is likely that similar storm surges also happen frequently. Therefore we will research other storm surge cases to detect the mechanism as well.

Acknowledgements

This report summarized the results of the cooperative research of “Numerical study

of the storm surges in the SIS caused by Typhoon Chaba in 2004" carried out by Meteorological Research Institute (MRI) and Takamatsu Local Observatory in 2004. It partly contains the results of the research project of "Study of processes of structural change of typhoons made landfall and the occurrence of strong wind, heavy rains, storm surge and high wave" in MRI. The authors would like to express their sincere gratitude to Dr. Ohno, the Director of the Takamatsu Local Observatory, for his helpful comments and continuous encouragement.

Some of data used in this research are collected in the "Urgent research about typhoons made landfall on Japan in 2004" of MRI, and the authors also show thanks to the organizations concerned for providing their data.

References

Arakawa, H. and M. Yoshitake, 1935：Report on the 'Muroto Taifu' in 1934, 347-361. (in Japanese)

Fujita, T., 1952：Pressure distribution within typhoon, Geophysical Magazine, 23, 437-451.

Japan Meteorological Agency, 2007, Outline of the Operational Numerical Weather Prediction at the Japan Meteorological Agency, 194pp, Available at "**http://www.jma.go.jp/jma/jma-eng/jma-center/nwp/outline-nwp/index.htm**"

JMA, 2000：Repot on the storm surges by Typhoon Bart (No.9918) in September 1999, Japan, Technical Report of the Japan meteorological Agency, 122, 168pp. (in Japanese)

Konishi, T., 1995：Storm surges in the western part of the Inland Sea, caused by Typhoon 9119 –analyses of tidal records, documents on flooding and field inspection-, Umi to Sora (SEA AND SKY), 70, 171-188. (in Japanese)

Konishi, T. and Y. Tsuji, 1995：Analyses of Storm Surges in the western part of the Seto Inland Sea of Japan caused by Typhoon 9119, Continental Shelf Res., 15, 1795-1823.

Kohno, N., 2000：The mechanism of storm surges caused by TY BART(9918) in 1999, KAIYO MONTHLY, 32, 763-770. (in Japanese)

Miyazaki, M., 2003：Research on Storm surges. The Examples and Mechanism, Seizando Press, 61-68. (in Japanese)